Anisotropic and mutable magnetization in Kondo lattice $CeSb_2$*

Yun Zhang(张云)[1,2], Xiegang Zhu(朱燮刚)[1], Bingfeng Hu(胡丙锋)[3], Shiyong Tan(谭世勇)[1], Donghua Xie(谢东华)[1], Wei Feng(冯卫)[1], Qin Liu(刘琴)[1], Wen Zhang(张文)[1], Yu Liu(刘瑜)[5,6], Haifeng Song(宋海峰)[5,6], Lizhu Luo(罗丽珠)[1], Zhengjun Zhang(张政军)[4], and Xinchun Lai(赖新春)[1,†]

[1] *Science and Technology on Surface Physics and Chemistry Laboratory, Mianyang* 621907, *China*
[2] *Department of Engineering Physics, Tsinghua University, Beijing* 100084, *China*
[3] *Key Laboratory of Neutron Physics, Institute of Nuclear Physics and Chemistry, China Academy of Engineering Physics, Mianyang* 621999, *China*
[4] *Key Laboratory of Advanced Materials (MOE), School of Materials Science and Engineering, Tsinghua University, Beijing* 100084, *China*
[5] *Laboratory of Computational Physics, Institute of Applied Physics and Computational Mathematics, Beijing* 100088, *China*
[6] *Software Center for High Performance Numerical Simulation, China Academy of Engineering Physics, Beijing* 100088, *China*

(Received 7 February 2017; revised manuscript received 8 March 2017; published online 20 April 2017)

We have systematically studied the behaviors of the resistivity and magnetization of $CeSb_2$ single crystals as a function of temperature and external field. Four anomalies in the resistivity/magnetization-versus-temperature curves are observed at low magnetic field. They are located at 15.5 K, 11.5 K, 9.5 K, and 6.5 K, corresponding to the paramagnetic–magnetically ordered state (MO), MO-antiferromagnetic (AFM), AFM–AFM, and AFM–ferromagnetic (FM) transitions, respectively. The anomaly at 9.5 K is only visible with $H \parallel [010]$ by magnetic susceptibility measurements, indicating that the AFM–AFM transition only happens along [010] direction in *ab*-plane. The four magnetic transitions are strongly suppressed by high external field. Finally, the field-temperature phase diagrams of $CeSb_2$ with different orientations of the applied field in *ab*-plane are constructed and indicate the highly anisotropic nature of the magnetization of $CeSb_2$.

Keywords: $CeSb_2$, electronic properties, magnetic properties

PACS: 71.27.+a, 51.60.+a **DOI:** 10.1088/1674-1056/26/6/067102

1. Introduction

Rare-earth compounds usually exhibit peculiar properties due to local magnetic moments, which originate from the partially filled *f*-shell.[1,2] The local moments interact with each other at low temperature, mediated by the Ruderman–Kittel–Kasuya–Yosida (RKKY) interaction.[3] When RKKY interaction is strong enough, the ground states of the rare-earth compounds become antiferromagnetically or ferromagnetically ordered,[4–6] ascribed to the lattice constant and Fermi vector of the systems. The light rare-earth diantimonides $ReSb_2$ crystallize in the layered orthorhombic structure.[7–10] Novel properties are reported in these quasi-two-dimensional compounds, such as charge density wave transitions in $LaSb_2$ and $PrSb_2$, and superconductivity in $LaSb_2$.[7,10,11] Besides, multiple magnetic properties, such as metamagnetic transitions (antiferromagnetic (AFM)), are observed in $CeSb_2$, $PrSb_2$, and $NdSb_2$ ($PrSb_2$) compounds.[10,12] Take the metamagnetic compound $CeSb_2$ for example, there are three anomalies in the resistivity/magnetization-versus-temperature curves, located at 15.5 K, 11.7 K, and 9.3 K. Except for the anomaly at 15.5 K, which is ascribed to the paramagnetic (PM) to ferromagnetic (FM) transition in *ab*-plane, the other two anomalies are not well identified.[7,10,13] Beyond that, due to the anticipated in-plane anisotropy of the metamagnetic transition, how the magnetization of $CeSb_2$ evolves as a function of temperature and external field with different field orientations is unclear.

In this paper, we have carefully studied the resistivity and magnetization of $CeSb_2$ single crystals as a function of temperature and external field. Upon cooling, four anomalies are observed, corresponding to the PM-magnetically ordered state (MO), MO–AFM, AFM–AFM, AFM–FM, respectively. In addition, the H–T phase diagrams of $CeSb_2$ with different orientations of the applied field are also constructed.

2. Materials and methods

High-quality single crystals $CeSb_2$ were grown using the self-flux method.[14,15] Ce and Sb raw materials (Alfa Aesar) were put together in alumina crucibles and sealed in quartz ampoules in a vacuum. Ampoules were heated to 950 °C in 3 hours, kept at 950 °C for 24 hours, then cooled down to 650 °C in 150 hours, and finally spun. The crystals grow as soft plates with the *c* axis perpendicular to the plates. The chemical compositions of the single crystals were determined by energy-dispersive x-ray spectroscopy. X-ray Laue diffraction and low energy electron diffraction (LEED)

*Project supported by the Science Challenge Project (Grant No. TZ2016004), the Dean Foundation of China Academy of Engineering Physics (Grant No. 201501040), and the National Basic Research Program of China (Grant No. 2015CB921303).

†Corresponding author. E-mail: Laixinchun@caep.cn

© 2017 Chinese Physical Society and IOP Publishing Ltd

experiments were performed to determine the crystal orientations of $CeSb_2$ single crystals. LEED experiments (electron energy = 90 eV) were performed in an ultra-high vacuum chamber ($< 10^{-10}$ mbar, 1 bar = 10^5 Pa) using the *in-situ* cleaved samples. The resistivity and magnetization measurements were performed with a Quantum Design Physical Property Measurement System (PPMS).

3. Results and discussions

The results of the resistivity measurements for $CeSb_2$ are presented in Fig. 1. The value of the residual resistance ratio (RRR = $\rho_{300\ K}/\rho_{2\ K} \sim 130$) is higher than the one previously reported[10] indicating the high quality of the samples. Upon cooling, the resistivity-versus-temperature (R–T) curve in Fig. 1(a) shows a broad hump at ~ 100 K accompanied by a decrease of the resistivity, resembling other typical Kondo lattice systems.[16,17] Besides, a dramatic decrease of the resistivity at ~ 15.5 K implies a phase transition,[18] accompanied by the decreased scattering rate and a much more ordered state. To trace the transition more clearly, the derivative of the resistivity $\mathrm{d}\rho/\mathrm{d}T$ curve is presented in the insert in Fig. 1(a). Except for the anomaly at 15.5 K, another three anomalies at 11.5 K, 9.5 K, and 6.5 K are also observed. The former three anomalies (15.5 K, 11.5 K, and 9.5 K) were reported previously.[10] and correspond to three magnetic transitions. Interestingly, we find a new anomaly at 6.5 K, which could be clearly observed in Figs. 1(a)–1(c). It is accompanied by an increase in resistivity, implying an enhancement of the electron scattering or a decrease of the density of state near the Fermi level. The onset temperatures of the four anomalies from the R–T curves all decrease and eventually vanish with increasing magnetic field, indicating that all the anomalies are related to magnetism. Figure 1(d) shows the field-dependent magnetoresistance of $CeSb_2$ with different temperatures. Two dramatic changes in resistivity as a function of applied field occur at low temperature. The first change at ~ 0.3 T emerges below 13 K, while the other one at ~ 2 T becomes evident below 16 K. By comparing the R–T curves and the magnetoresistance curves in Figs. 1(b)–1(d), we find that the changes of the magnetoresistance at ~ 0.3 T and ~ 2 T seem to be related to the magnetic transitions at 11.5 K and 15.5 K, respectively. First, the change at 0.3 (2) T in the magnetoresistance curve emerges below 13 (16) K, consistent with onset temperature of the anomaly at 11.5 (15.5) K in the R–T curve. Second, the anomaly at 11.5 (15.5) K in the R–T curve disappears when the external field is above 0.3 (1.8) T, in agreement with the onset magnetic field of the change at 0.3 (2) T in the magnetoresistance curve.

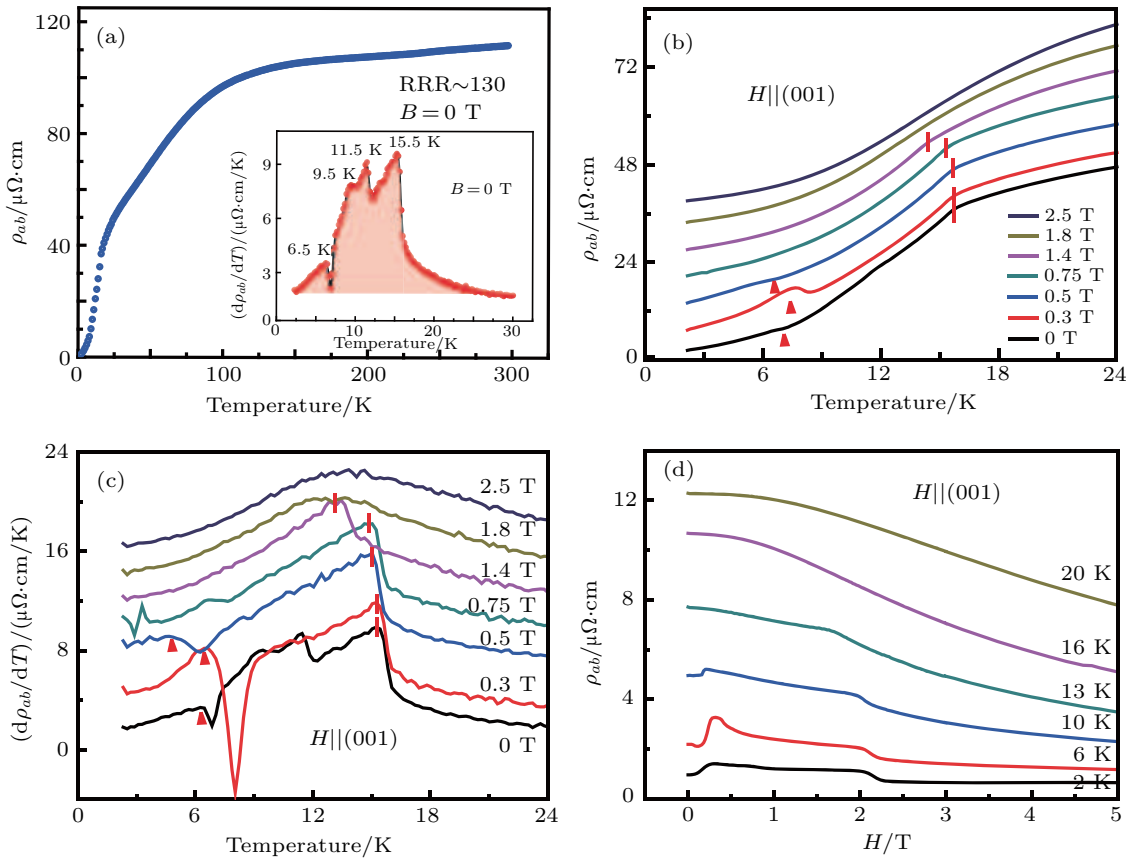


Fig. 1. (color online) Resistivity measurements of $CeSb_2$ with $I \parallel (001)$. (a) Zero-field resistivity of $CeSb_2$. The insert is the temperature derivative of the resistivity at low temperature. (b) and (c) Resistivity of $CeSb_2$ and the corresponding temperature derivative at different magnetic fields. The red triangles and vertical bars are marks of the anomalies at 6.5 K and 15.5 K, respectively. (d) Field-dependent magnetoresistance for $CeSb_2$ at different temperatures with $H \parallel (001)$. The curves in Figs. 1(b)–1(d) are shifted for a better view.

Due to the tiny discrepancy between a and b axes ($a \sim 0.6295$ nm, $b \sim 0.6124$ nm) in ab-plane,[19] a possible anisotropy of the susceptibility is anticipated. The crystal structure of $CeSb_2$ is exhibited in Figs. 2(a1)–2(a2), consisting of a layered structure along c axis and an orthorhombic structure in ab-plane. Figure 2(a3) shows the LEED pattern of the as-grown facet of $CeSb_2$ single crystal. The bright spots in the square-like lattice reflect the pristine 1×1 surface, indicating the high quality of $CeSb_2$ single crystals and their in-plane crystal orientations. However, it seems difficult to distinguish the [010] and [100] directions for the tiny difference between the lattice constants along the two directions. We systematically study the magnetic properties of $CeSb_2$ with different external field orientations in (001) plane. Take the result of magnetization with $H \parallel [010]$ for example—complicatedly magnetic properties of $CeSb_2$ as a function of temperature and magnetic field are observed. First, we focus on the anomaly at ~ 15.5 K in Figs. 2(b)–2(c). The onset temperature of this anomaly goes down with increasing applied field and finally disappears at $\sim$4 T. This feature agrees well with the anomaly at 15.5 K in resistivity in Fig. 1 and is ascribed to the PM–MO transition. However, the behavior of the anomaly at 15.5 K is different from the ferromagnet $Na_{0.55}CoO_2$ as a function of magnetic field.[20] Second, the value of magnetic susceptibility sharply decreases at 11.5 K with $H = 0.1$ T. When the applied field is in the range of 0.1 T$< H <$ 0.7 T, the sudden turning point at 11.5 K splits into two. The onset temperatures of the two turning points both decrease with increasing applied field until 1.5 T, where the turning points totally disappear. We suppose that $CeSb_2$ compound goes through two AFM transitions in the small temperature range. One is an MO–AFM transition and the other is an AFM–AFM transition. The two transitions are suppressed under high external field, similar to the two anomalies at 11.5 K and 9.5 K in resistivity curves. Third, when the external field is smaller than 0.5 T, the magnetic susceptibility curves start to increase below 8 K and possess the largest slopes at about 6.5 K. This temperature agrees well with the new anomaly in resistivity curve in Fig. 1 [panels (a)–(c)]. Therefore, we speculate that an AFM–FM transition happens at about 6.5 K and seems to gap the Fermi surface partially, quite similar to other spin density wave compounds.[21] Up to now, we almost complete the ground state of $CeSb_2$ compound under low temperature and low applied field. Complicated PM–MO (15.5 K)–AFM (11.5 K)–AFM (9.5 K)–FM (6.5 K) phase transitions occur, whereas the situation starts to change with higher applied field. When the applied field is in the range of 1.5 T$< H <$ 4 T, only PM–MO transition remains with an anomaly at $\sim$ 15 K in susceptibility curves. When the magnetic field is above 4 T, the anomaly at $\sim$ 15 K disappears in Fig. 2(c).

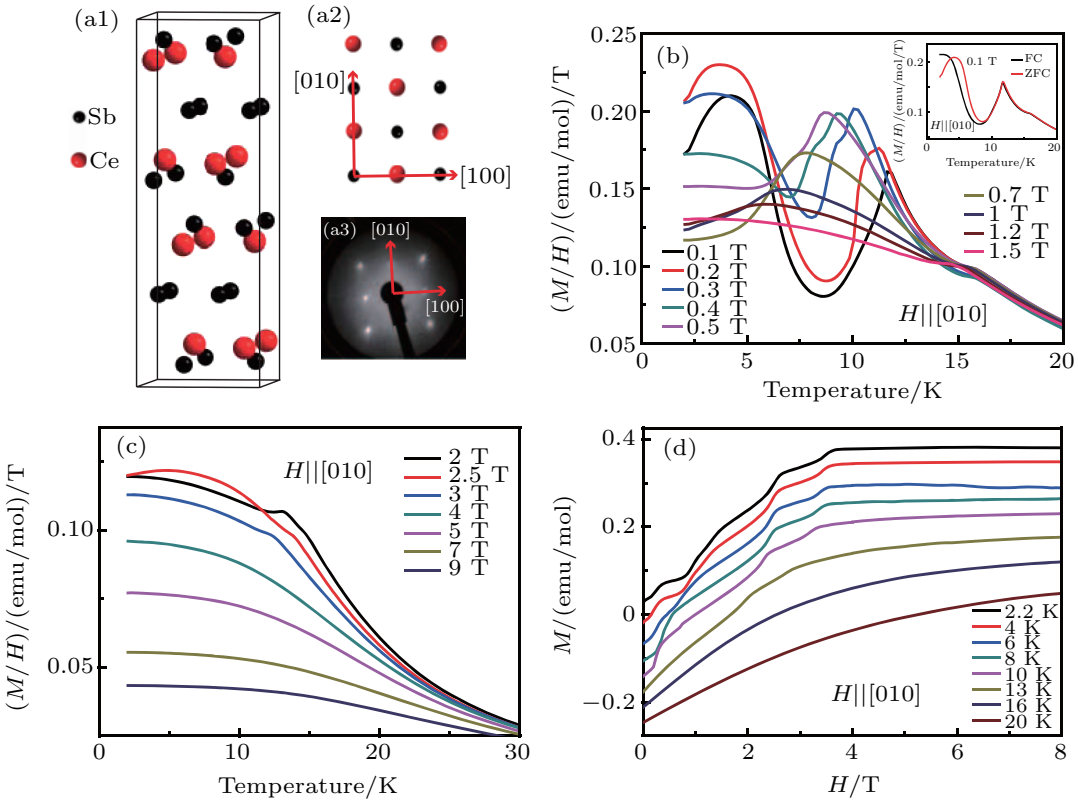


Fig. 2. (color online) Magnetic susceptibility measurements of $CeSb_2$ with $H \parallel [010]$. (a1) Side view of the crystal structure of $CeSb_2$. (a2) top view of crystal surface of $CeSb_2$ along [001] direction. (a3) LEED pattern for the as-grown facet of $CeSb_2$ single crystal. The red arrows indicate the in-plane [100] and [010] directions. (b)–(c) Zero-field cooling (ZFC) magnetic susceptibility of $CeSb_2$ with different magnetic fields along [010] direction. The insert in Fig. 2(b) is the results of the ZFC and FC magnetic susceptibility measurements. (d) Magnetization isotherms for $CeSb_2$ at different temperatures with $H \parallel [010]$. The curves in Fig. 2(d) are shifted for a better view.

Several metamagnetic transitions of $CeSb_2$ are observed at low temperature in the magnetization isotherms in Fig. 2(d). The step-like changes of the magnetization as a function of external field at 2.2 K are gradual and may be due to the rotations of the spins. The first and third metamagnetic transitions at ~ 0.3 T and 2.3 T are consistent with the sudden jumps in the magnetoresistance curves in Fig. 1(d), which are related to the MO–AFM (11.5 K) and PM–MO (16 K) transitions closely. However, the other two transitions located at 1 T and 3.5 T in Fig. 2(d) seem inconsistent with the magnetoresistance curve. In addition, the shape of the $M(H)$ curve at 2.2 K is different from the literature[10] and the shapes of the other $M(H)$ curves with external field along other directions in Fig. 3. It results from the in-plane anisotropy of the metamagnetic transitions (discussed in Fig. 4).

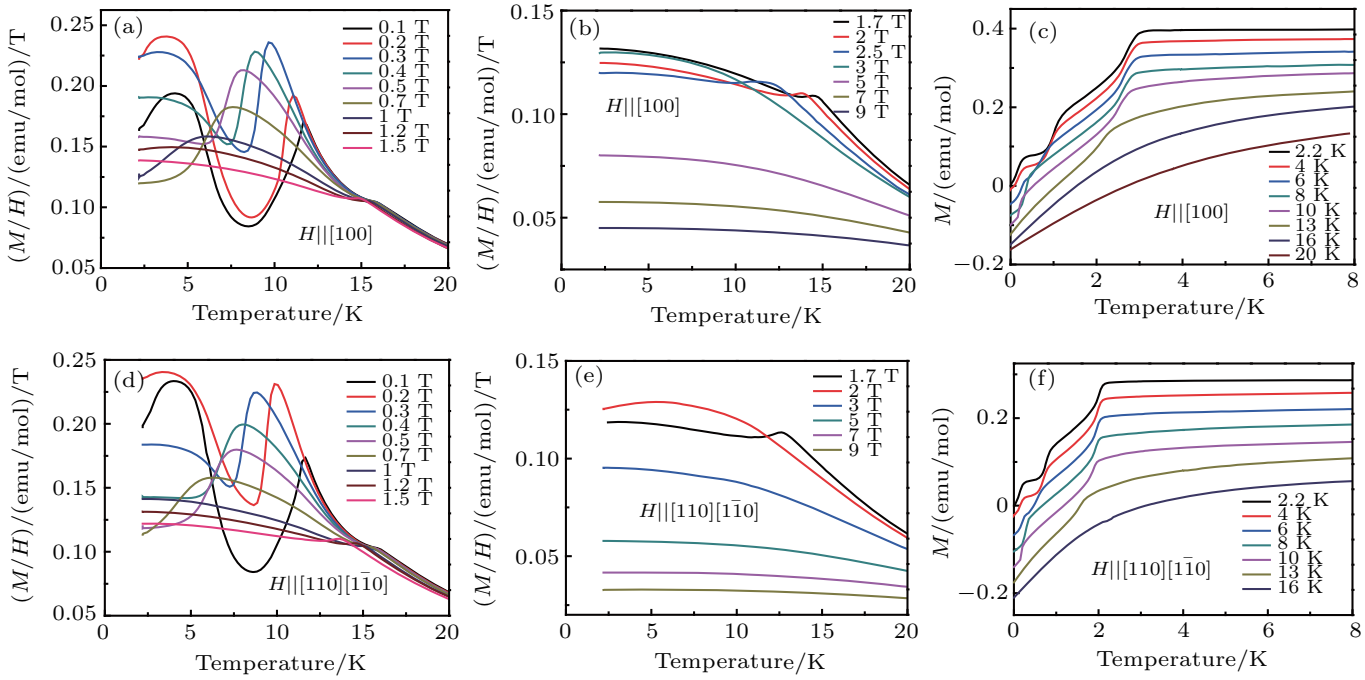


Fig. 3. (color online) Magnetic susceptibility measurements of $CeSb_2$ with $H \parallel [100]$, [110], and [1$\bar{1}$0]. (a) and (b) ZFC magnetic susceptibility of $CeSb_2$ with different magnetic fields along [100] direction. (c) Magnetization isotherms for $CeSb_2$ at different temperatures with $H \parallel [100]$. (d)–(e) ZFC magnetic susceptibility of $CeSb_2$ with different magnetic fields along [110] and [1$\bar{1}$0] directions. (f) Magnetization isotherms for $CeSb_2$ at different temperatures with $H \parallel [110]$ and [1$\bar{1}$0]. The curves in Fig. 3(c) and Fig. 3(f) are shifted for a better view.

When the external field is along [100] direction, some changes in the magnetic susceptibility curves occur in Figs. 3(a)–3(c). The neighboring two AFM transitions with $H \parallel [010]$ around 11.5 K merge to one in Fig. 3(a). The behavior of the metamagnetic transitions in Fig. 3(c) also becomes simpler. Only three metamagnetic transitions remain. The PM–MO and MO–AFM transitions with $H \parallel [100]$ are totally suppressed when external field is larger than 2.5 T and 1.2 T, respectively. When the magnetic field turns to the [110] or [1$\bar{1}$0] direction, the PM–MO and MO–AFM transitions are totally suppressed when the external field is larger than 1.7 T and 1 T, respectively. The metamagnetic transitions at low temperature in Fig. 3(c) and Fig. 3(f) are similar to each other. Only the absolute values of the parameters, such as the saturation magnetization and the critical magnetic field, are different.

The anisotropy of the metamagnetic transitions is presented in Fig. 4(a). The magnetizations with $H \parallel [110]$ and $H \parallel [1\bar{1}0]$ nearly coincide with each other. However, the saturation magnetization increases to $M_{100} = 0.99\sqrt{2}M_{110}(M_{010} = 0.92\sqrt{2}M_{110})$ when the orientation of the magnetic field is along [100] ([010]) direction. The values of saturation magnetization with $H \parallel [100]$ and [010] are larger than the values with $H \parallel [110]$ and [1$\bar{1}$0], whereas they also need larger magnetic fields for magnetizations to be saturated with $H \parallel [100]$ and [010]. Consequently, it is quite difficult to define the easy axis of this compound in (001) plane. For Kondo lattice systems, RKKY interaction is significant for the formation of the magnetic ground state. Because RKKY interaction decays as $/r^3$,[22] where r is the distance between the interacting magnetic moments, the ratio of the RKKY interaction strengths between $a_{0.6295\ \mathrm{nm}}$ and $b_{0.6124\ \mathrm{nm}}$ axes in ab-plane is $\mathrm{RKKY}_{0.6295}/\mathrm{RKKY}_{0.6124} = (0.6124/0.6295)^3 = 0.92$, consistent with the ratio of the magnetic susceptibility along the two directions M_{100}/M_{010}=0.923 at 0.1 T and 2.2 K under FC process. When the external field is smaller than 0.3 T, $CeSb_2$ compound does not go through the first metamagnetic transition and can be regarded in the ground state. Therefore, we speculate that RKKY interaction is dominated in this low magnetic field region and consequently, the [010] ([100]) direction corresponds to the $b_{0.6124\ \mathrm{nm}}$ ($a_{0.6295\ \mathrm{nm}}$) axis.

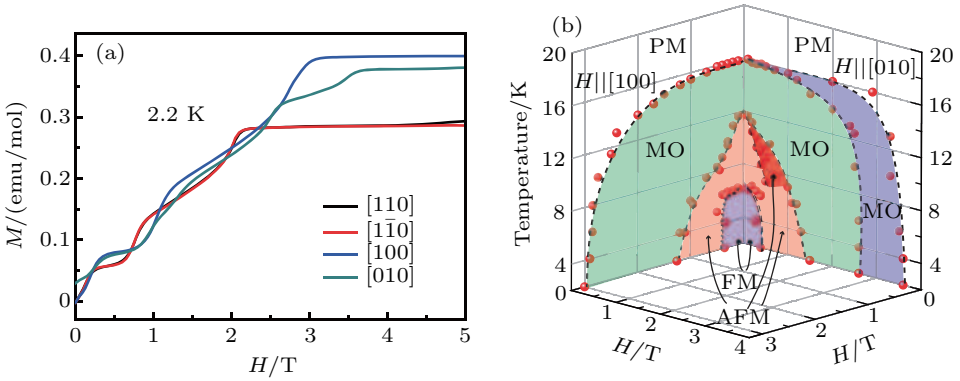


Fig. 4. (color online) Field-temperature phase diagrams of $CeSb_2$. (a) In-plane magnetization isotherms for $CeSb_2$ with external field along different orientations at 2.2 K. (b) H–T phase diagrams of $CeSb_2$ with external field along different orientations. The phase diagram with $H \parallel [100]$ is similar to the ones with $H \parallel [100]$ and $[1\bar{1}0]$. Only the absolute values of the parameters, such as the saturation magnetization, are different.

Based on the measurements of the magnetization as a function of temperature and magnetic field in Fig. 2 and Fig. 3, complete H–T phase diagrams of $CeSb_2$ single crystal with magnetic field along (001) plane are exhibited in Fig. 4(b). When the external field is along [100] ([110] $[1\bar{1}0]$) direction, the system shows at least three magnetically ordered states, including an FM, an AFM, and an MO state in the left plane in Fig. 4(b). If the applied field is turned to [010] direction, namely the $a_{0.6124\ \mathrm{nm}}$ axis, the phase diagram becomes more complicated, consisting of an FM, two AFM, and two MO states in the right plane in Fig. 4(b).

4. Conclusions

In summary, we have studied the resistivity and magnetization of $CeSb_2$ as a function of temperature and external field. Four anomalies in the resistivity and magnetization curves, located at 15.5 K, 11.5 K, 9.5 K, and 6.5 K, are observed. They correspond to the PM–MO, MO–AFM, AFM–AFM, and AFM–FM transitions, respectively. In addition, the H–T phase diagrams of $CeSb_2$ with different orientations of the applied field are constructed.

References

[1] Christian P 2009 *Rev. Mod. Phys.* **81** 1551
[2] Stewart G R 1984 *Rev. Mod. Phys.* **56** 755
[3] Coleman P 2007 *Handbook of Magnetism and Advanced Magnetic Materials* (John Wiley & Sons, Ltd.) p. 95
[4] Hegger H, Petrovic C, Moshopoulou E G, Hundley M F, Sarrao J L, Fisk Z and Thompson J D 2000 *Phys. Rev. Lett.* **84** 4986
[5] Sidorov V A, Bauer E D, Frederick N A, Jeffries J R, Nakatsuji S, Moreno N O, Thompson J D, Maple M B and Fisk Z 2003 *Phys. Rev. B* **67** 224419
[6] Pan Z Y, Cao C D, Bai X J, Song R B, Zheng J B and Duan L B 2013 *Chin. Phys. B* **22** 056102
[7] Luccas R F, Fente A, Hanko J, Correa-Orellana A, Herrera E, Climent-Pascual E, Azpeitia J, Pérez-Castañeda T, Osorio M R, Salas-Colera E, Nemes N M, Mompean F J, García-Hernández M, Rodrigo J G, Ramos M A, Guillamón I, Vieira S and Suderow H 2015 *Phys. Rev. B* **92** 235153
[8] Kagayama T, Uwatoko Y, Bud'ko S L and Canfield P C 2005 *Physica B: Condens. Matter* **359-361** 320
[9] Kagayama T, Oomi G, Bud'ko S L and Canfiel P C 2000 *Physica B: Condens. Matter* **281** 90
[10] Bud'ko S L, Canfiel P C, Mielke C H and Lacerda A H 1998 *Phys. Rev. B* **57** 13624
[11] Guo S, Young D P, Adams P W, Wu X S, Chan J Y, McCandless G T and DiTusa J F 2011 *Phys. Rev. B* **83** 174520
[12] Kagawa A, Kagayama T, Oomi G, Mitamura H, Goto T, Can"eld P C and Bud'ko S L 2000 *Physica B: Condens. Matter* **281** 124
[13] Canfield P C, Thompson J D and Fisk Z 1991 *J. Appl. Phys.* **70** 5992
[14] Canfield P C and Fisk Z 1992 *Philos. Mag. B* **65** 1117
[15] Xie D H, Zhang W, Liu Y, Feng W, Zhang Y, Tan S Y, Zhu X G, Chen Q Y, Liu Q, Yuan B K and Lai X C 2016 *Chin. Phys. B* **25** 047502
[16] Pagliuso P G, Moreno N O, Curro N J, Thompson J D, Hundley M F, Sarrao J L, Fisk Z, Christianson A D, Lacerda A H, Light B E and Cornelius A L 2002 *Phys. Rev. B* **66** 054433
[17] Jourdan M, Zakharov A, Foerster M and Adrian H 2004 *Phys. Rev. Lett.* **93** 097001
[18] Zhang X D, Wu W, Zheng P, Wang N L and Luo J L 2012 *Chin. Phys. B* **21** 017402
[19] Wang R and Steinfink H 1967 *Inorg. Chem.* **6** 1685
[20] Wang C, Chen X, Wu T, Luo X, Wang G and Luo J 2006 *Phys. Rev. Lett.* **96** 216401
[21] Grüner G 1994 *Rev. Mod. Phys.* **66** 1
[22] Shishido H, Shibauchi T, Yasu K, Kato T, Kontani H, Terashima T and Matsuda Y 2010 *Science* **327** 980